Interpretation of Anomeric Effect in the N−C−N Unit with the Quantum Theory of Atoms in Molecules

Keiamars Eskandari,[†] Antonio Vila, and Ricardo A. Mosquera*

Departamento de Química Física, Universidade de Vigo, Facultade de Química, 36310-Vigo, Galicia, Spain

Received: May 16, 2007; In Final Form: June 28, 2007

The conformational preferences of six model compounds for the N−C−N anomeric unit (methanediamine, 2,2-propanediamine, *N*,*N*,*N*′,*N*′-tetramethyl-methanediamine, 1,3-dizacyclohexane, 1,3,5-triazacyclohexane, and 2-aminopiperidine) were analyzed within the framework of the Quantum Theory of Atoms in Molecules. The relative stabilization of the conformers is related to two factors: (i) the reduction of the electron population experienced by the hydrogens of the central methylene when they display more gauche arrangements to lone pairs (*lp*) and (ii) the reduction of the electron population of aminic hydrogens when the corresponding N−H bond is in a parallel arrangement to the lone pair of another N. The former depletion takes place in *lp*−N−C−N antiperiplanar dispositions, whereas the latter is shown in *lp*−N−C−N gauche arrangements. Therefore, we can say that the electron density removed from the central hydrogens is moved to an aminic one on going from an antiperiplanar to a gauche disposition of a *lp*−N−C−N unit. The relative energies of aminic and central hydrogens in the conformer series is the main factor determining the conformational preference. In contrast to what happens in O−C−O containing compounds (where both *N*(H) depletions take place in the O−C−O−H gauche dispositions), the stabilization gained by N and C atoms plays a secondary role. This is in line with a general trend exhibited by hydrogens as the most available (less energy cost) atomic basins for receiving or providing electron density along a chemical change. It also explains why the anomeric conformational stabilization due to the N−C−N units is significantly less than that of the O−C−O− units. Moreover, the variations of electron population due to conformational changes are not in keeping with the stereoelectronic model of the anomeric effect, as was previously found for diverse molecules containing the O−C−O anomeric unit.

Introduction

The conformational preference for a gauche arrangement of the R−Y−C−Z fragment, where Y is an atom bearing at least one lone pair of electrons, *lp*, and Z is an element more electronegative than C, is known as the generalized anomeric effect.[1−4] Several theoretical models have been proposed to explain this conformational trend. Although dipolar electrostatic interactions were first considered as its origin,[5] they failed to explain the conformational preferences observed for some compounds,[6,7] and a different interpretation (hereafter referred to as the stereoelectronic model, SM) based on electron delocalization became widely accepted. In its initial proposition, which is just a rough description of its present version, the SM considers that the conformational stabilization arises from the delocalization of one of Y's *lp*s into the antibonding orbital C−Z, σ^*_{C-Z}, that takes place when the *lp*−Y−C−Z unit adopts an antiperiplanar arrangement.[8] This electron transfer is denoted as $n_Y \rightarrow \sigma^*_{C-Z}$. Natural bond orbital (NBO) studies have shown that other orbital and bond−antibond interactions, as well as steric and electrostatic effects, have to be taken into account, with a relative importance that depends on the system under consideration.[6,9−12] If we concentrate on the N−C−N anomeric unit, previous NBO studies have indicated that $n_N \rightarrow \sigma^*_{C-N}$ orbital interactions are the dominant contributions for explaining the conformational preference.[12−15] Therefore, the SM (considering only these interactions) is still usually employed to rationalize the anomeric effect in linear and cyclic compounds where no other anomeric moieties but N−C−N are present.

On the other hand, the conformational preferences of two model compounds for the O−CH_2−O anomeric unit (methanediol and dimethoxymethane) were analyzed in a recent paper[16] within the framework of the quantum theory of atoms in molecules (QTAIM).[17,18] This analysis has shown that the variations experienced by atomic electron populations because of conformational changes are not in line with the SM. On the contrary, these variations are the basis of a new interpretative model of the anomeric effect. According to it, the characteristic stabilization of the gauche conformers of methanediol and dimethoxymethane is accompanied by a progressive reduction of the electron population of the hydrogens of the central methylene, H^C, as the number of their gauche interactions to the *lp*s rises. The electron population removed from H^Cs in the gauche conformers is gained by atoms of larger atomic numbers, which results in a more negative molecular energy. It has to be noticed that another previous QTAIM study on dimethoxymethane also concluded that the anomeric effect is not derived from a differential interaction of a lone pair with an antiperiplanar CH_2−O bond.[19] That work did not provide an alternative interpretation for the anomeric effect. Moreover, the same trends observed for QTAIM atomic electron populations of methanediol and dimethoxymethane were also found in other branched and cyclic compounds that contain the O−C−O unit.[20]

This work aims to check if the new interpretation proposed for the anomeric effect in O−C−O containing systems can be

* Corresponding author. E-mail: mosquera@uvigo.es.
[†] On leave from: Chemistry Department, College of Sciences, Shiraz University, Shiraz, 71454 Iran.

10.1021/jp073801y CCC: $37.00
Published on Web 08/09/2007

extended to compounds with the N−C−N unit or if it needs some modification. To this end, we have carried out a QTAIM analysis for the conformers of six model compounds. They include three linear compounds: methanediamine (**MDA**) and those resulting from replacing central and aminic hydrogens with methyl groups, 2,2-propanediamine (**PDA**), and *N*,*N*,*N*′,*N*′-tetramethylmethanodiamine (**TMMDA**). Three cyclic molecules were also considered: 1,3-diazacyclohexane (**DAC**), 1,3,5-triazacyclohexane (**TAC**), and 2-aminopiperidine (**APP**). For the simplest molecule, **MDA**, we have also analyzed how the QTAIM atomic electron populations evolve along the internal rotations. Also, for **MDA**, we have checked that the structural trends obtained for the conformational process do not change with the computational level.

Computational Details

All the conformers of five molecules (**MDA**, **PDA**, **DAC**, **TAC**, and **APP**), and the ***tt*** and ***gg*** conformers of **TMMDA**, were fully optimized at the B3LYP/6-311++G(2d,2p) 6d level using the *Gaussian 03* program.[21] The harmonic vibrational frequencies were also calculated to characterize the optimized stationary points. The integrations over the atomic basins of all the conformers were carried out using the AIMPAC program series.[22,23] The same study was also performed for **MDA** at MP2 and HF levels with the same basis set.

The conformers of all the N−C−N models are named by an acronym that indicates the approximate values of the *lp*−N−C−N dihedral angles beginning with that where the *lp* belongs to N_1. In these acronyms, ***t*** and ***g*** denote, respectively, antiperiplanar and gauche arrangements. When necessary, the distinction between gauche arrangements with positive and negative main dihedral angles is made denoting the latter as ***g′***. It must be stressed that conformational nomenclature in O−C−O models refers to H−O−C−O dihedral angles. Thus, **MDA-*tt*** represents the conformation with the highest number of *lp*−Y−C−H^C gauche arrangements (four), as well as ***gg*** in methanediol (four).

The summations of electron atomic populations, $N(\Omega)$, and atomic energies, $E(\Omega)$, for the conformers match the total number of electrons and the total molecular energy within 0.001 au and 3 kJ mol^{-1}, respectively. No atom of these conformers was integrated with $L(\Omega)$ differing from zero (the value of ideal atom delimitation)[14] by more than 2×10^{-3} au. According to the slopes of the linear relationships between the computed $N(\Omega)$ and $L(\Omega)$ that were previously found,[24−28] the error in $N(\Omega)$ is estimated to be less than $\pm 2.5 \times 10^{-3}$ au for carbons and nitrogens and less than $\pm 3 \times 10^{-4}$ au for hydrogens. Summations of $N(\Omega)$ and $E(\Omega)$ values obtained for restricted optimized structures along the internal rotational paths of **MDA** match the corresponding molecular properties within 2.10^{-4} au and 1 kJ mol^{-1}, respectively.

QTAIM atomic energies, $E(\Omega)$, are usually calculated as the product of the atomic electronic kinetic energy, $K(\Omega)$, and $1 - \gamma$, γ being the molecular virial ratio.[17,18] This avoids the computation of terms that involve the simultaneous integration on two atomic basins: Coulomb electronic repulsion and exchange energy. Although nothing assures that the value of the molecular virial ratio can be used as the atomic virial ratio,[29] it is generally convenient, as shown by Cortes-Guzmán and Bader,[30] to work with $E(\Omega)$ values computed with electron distributions that follow very approximately the virial theorem, such as those obtained with the self-consistent virial scaling (SCVS)[31] method. In fact, this is crucial to avoid undesirable artifacts when comparing $E(\Omega)$ values computed for molecules of different sizes,[30] what our group had named the "size effect" (that is, the molecular size dependence observed for the atomic energy of a set of nearly transferable atoms).[24,26,29] Nevertheless, it has been proven that relative atomic energies obtained for conformers of the same molecule are scarcely affected by small changes in γ.[16] In this case, the variations of γ ratios among the conformers of the same molecule (and restricted optimized structures computed for **MDA**) do not exceed 9×10^{-6}. Taking into account $K(\Omega)$ values, we can estimate that the effects on relative atomic energies, $\Delta E(\Omega)$, are below 1.3 kJ mol^{-1} for N and C atoms and 0.02 kJ mol^{-1} for hydrogens. As this work is only concerned with relative atomic energies of conformers, whose variations exceed these confidence limits, we have not made use of SCVS optimizations.

The significant effects that basis sets can introduce in QTAIM properties of polar bonds, previously described by Henn et al.,[32] were shown to affect the absolute $N(\Omega)$ and $E(\Omega)$ quantities but were negligible upon relative $\Delta N(\Omega)$ and $\Delta E(\Omega)$ values, which followed the same patterns with 10 different basis sets.[16] As our study is based upon relative $\Delta N(\Omega)$ and $\Delta E(\Omega)$ values, we have only used one basis set.

TABLE 1: Total Electronic Molecular Energies for Diverse Conformers of Molecules Studied Here[a]

	computational level[b]	***tt***	***tg***	***gg***	***gg′***
MDA	HF	−150.30281	1.4	2.0	17.6
	B3LYP	−151.27567	2.5	4.6	*c*
	MP2	−150.30200	1.5	2.2	*c*
MDO[d]	HF	29.7[e]	13.4	−189.98152	12.4
	B3LYP	32.1[e]	*f*	−191.02647	11.2
	MP2	32.4	13.9	−190.58376	11.6
PDA	B3LYP	−229.93500	0.2	0.2	15.5
TMMDA[g]	B3LYP	−308.54538		−19.1	
DAC	B3LYP	−268.02861	0.4		10.6
		ttt	*ttg*	*tgg′*	*gg′g*
TAC	B3LYP	−284.06982	3.4	16.4	39.5

[a] Absolute values (au) for conformers with the largest number of *lp*−Y−C−H^C gauche arrangements and relative values (kJ mol^{-1}) for the rest. [b] All calculations were carried out with the standard 6-311++G(d,p) 6d basis set. [c] ***gg′*** was not found as a conformer for **MDA** at the B3LYP and MP2 levels. [d] **MDO** (methanediol) results taken from ref 16. [e] **MDO-*tt*** was obtained as a transition state at the HF and B3LYP levels. [f] ***tg*** was not obtained as a stationary point at the HF level for **MDO**. [g] Only ***tt*** and ***gg*** conformers were studied for **TMMDA**.

Results and Discussion

Methanediamine. Three conformers were obtained for **MDA** (**MDA-*tt***, **MDA-*tg***, and **MDA-*gg***) at the B3LYP and MP2 levels with the 6-311++G(2d,2p) 6d basis sets. The **MDA-*gg′*** conformation is found to be a relative minimum of high energy (ΔE > 16 kJ mol^{-1}) on most of HF (HF/6-311++G(2d,2p) included) and molecular mechanics[33] potential energy surfaces, whereas it is not a stationary point for most of the MP2 and DFT calculations hitherto performed for this compound.[12]

There is no experimental structural study available for this molecule, but **MDA-*tt*** is found to be the most stable conformer at all the computational levels here and previously considered.[12,34,35] When the relative energies of the conformers (Table 1) are compared with those presented in the analogous compound bearing the anomeric O−C−O unit (methanediol), we observed that they are significantly reduced in **MDA** (e.g., the MP2 relative energy of ***tg*** is 13.9 kJ mol^{-1} in methanediol and 1.5 kJ mol^{-1} in **MDA**). Taking into account the definition of the anomeric effect in the Introduction, the small relative energies of conformers with less H−N−C−N gauche arrange-

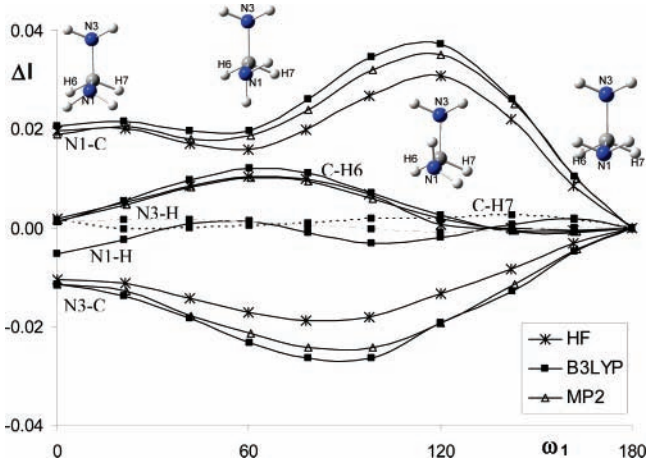

Figure 1. Evolution of selected bond lengths (Å) along the internal rotation of methanediamine (represented by $\omega_1 = lp{-}N_1{-}C_2{-}N_3$, in deg) with $N_1{-}C_2{-}N_3{-}lp$ in antiperiplanar ($\omega_2 = t$) arrangement.

ments (**MDA-*gg***) indicate that the anomeric effect in **MDA** is less intense than in methanediol and weaker in N−C−N units than in O−C−O ones. This conclusion can also be inferred from the evolution of molecular energies along the internal rotation. Thus, the rotational barrier of methanediol is computed to be 32.1 kJ mol^{-1} at the B3LYP level, whereas it is 13.4 kJ mol^{-1} in **MDA** (Figure S1, Supporting Information).

C−N bond lengths (computed at any computational level) display well-known anomeric geometry trends along the internal rotation of **MDA** (Figure 1), shrinking N1−C and lengthening N3−C for the *lp*−N1−C2−N3 antiperiplanar arrangement. This behavior was interpreted in terms of $N1^{+}{=}C2{\cdots}N3^{-}$ resonance forms associated with the most favorable geometry disposition for the $n_{N1} \rightarrow \sigma^*_{C2-N3}$ transference. Nevertheless, the same argument indicates that the longest N1−C2 bond length and the shortest N3−C2 bond length should appear at $\omega_1 = 0°$, whereas they are found as, respectively, 120 and 80°. We also observe that whereas the C−H bond length of the hydrogen whose steric repulsions are almost the same during the rotation (H_7) is nearly constant, the other C−H distance (C−H_6) displays a significant variation.

The QTAIM theory characterizes the chemical bonds using the values of several quantities computed at the (3,−1) critical points of the electron density, which are named bond critical points (BCPs).[17,18] The evolution of most of these properties (electron density, ρ_b, laplacian of the electron density, $\nabla^2\rho_b$, and total energy density, H_b) along the series of conformers is linearly correlated with that of the bond length, as was previously observed.[36] Therefore, their evolutions do not contradict the main prediction of SM. Thus, we can observe that the ρ_b values of N1−C2 and C2−N3 display, respectively, their maximum and minimum along the ω_1 rotation for the *lp*−N1−C2−N3 antiperiplanar arrangement (Figure 2), which is in line with a hypothetical $^{+}N1{=}C2{\cdots}N3^{-}$ resonance structure due to $n_{N1} \rightarrow \sigma^*_{C2-N3}$ transference.

$\Delta N(\Omega)$ values for the **MDA** conformers (Figure 3) show that an increased number of $H^C{-}C{-}N{-}lp$ gauche arrangements result, as found in O−C−O containing compounds,[16] in diminished $N(H^C)$ populations (0.032 au less in **MDA-*tt*** than in **MDA-*gg***). $\Delta N(H^C)$ values correspond indeed to the largest electron population variations observed among conformers, as was found for O−C−O anomeric compounds. Also, when the number of $H^C{-}C{-}N{-}lp$ gauche arrangements only varies for one of the H^C atoms (H_6 in **MDA-*tg***), this is the only one whose

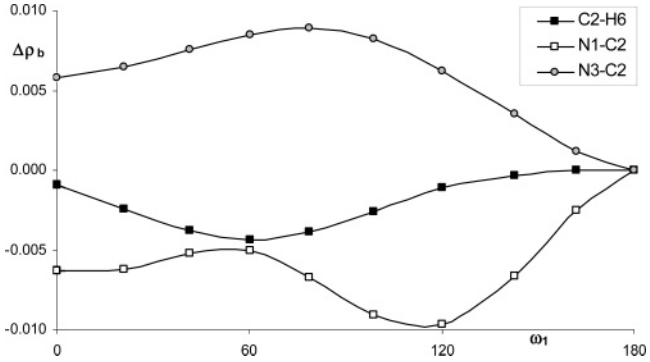

Figure 2. Evolution of ρ_b values (au) for selected bonds along the internal rotation of methanediamine (represented by $\omega_1 = lp{-}N_1{-}C_2{-}N_3$, in deg) with $N_1{-}C_2{-}N_3{-}lp$ in antiperiplanar ($\omega_2 = t$) arrangement.

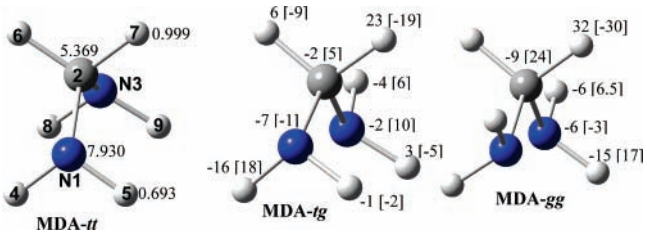

Figure 3. Structure and atom numbering of conformers of methanediamine (**MDA**). Absolute $N(\Omega)$ values (for **MDA-*tt***) are in au. Relative atomic electron populations, $\Delta N(\Omega)$ (for **MDA-*tg*** and **MDA-*gg***), are in au and multiplied by 10^3. $\Delta E(\Omega)$ values relative to atomic energies in **MDA-*tt*** are shown in brackets (kJ mol^{-1}). All values were obtained from B3LYP/6-311++G(2d,2p) calculations. **MDA-*tt***, **MDA-*tg***, and **MDA-*gg*** full optimized geometries display, respectively, C_{2v}, C_1, and C_2 symmetries.

$N(\Omega)$ value becomes significantly affected ($\Delta N(H_6)$ is 0.023 au, while $\Delta N(H_7)$ is 0.006 au).

An additional fact has to be taken into account to rationalize the whole set of $\Delta N(\Omega)$ values presented in Figure 3: 1,4-parallel dispositions of N−H bonds to a *lp* of the other nitrogen diminishes the atomic population of that aminic hydrogen.

The increased electron−electron repulsions associated with parallel disposition of N−H bonds to the nitrogen *lp* explain why N(H4) diminishes in **MDA-*tg*** and why both N(H4) and N(H5) diminish in **MDA-*gg*** with regard to **MDA-*tt*** in both cases. It should be noted that the largest number of $lp{-}X{-}C{-}H^C$ (X═O) gauche dispositions and that of parallel $lp{-}X{\cdots}X'{-}H^X$ arrangements take place in the same conformers of methanediol (the number of both relative orientations increases in the series ***gg*** > ***tg*** > ***tt***). In contrast, parallel $lp{-}X{\cdots}X'{-}H^X$ (X═N) arrangements are present in **MDA-*gg*** but not in **MDA-*tt***, whereas the largest number of $lp{-}X{-}C{-}H^C$ gauche dispositions corresponds to **MDA-*tt*** (Figure S2, Supporting Information). Therefore, both effects remove electron density from central and hydroxilic hydrogens in the most stable conformer of methanediol (**MDO-*gg***), whereas they act in a different way in **MDA** conformers. Thus, looking at **MDA-*gg*** with regard to **MDA-*tt***, some electron density should be expelled from two H^N atoms as the corresponding $N{-}H^N$ bonds become parallel to $N{-}lp$, and at the same time, some electron density should be accepted by H^C atoms because they display less $lp{-}N{-}C{-}H^C$ gauche dispositions. If we also consider that N is less electronegative than O, everything favors that the electron density lost by H^C in the most stable conformer of **MDA** is not only gained by heavy atoms but also by other hydrogens becoming much more distributed in the whole molecule than

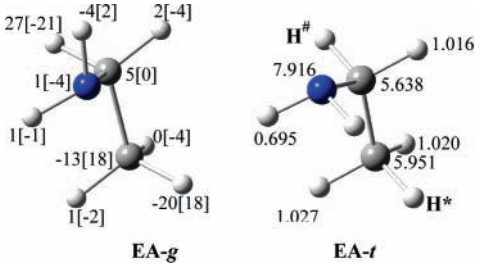

Figure 4. Relative atomic electron populations, $\Delta N(\Omega)$ (in au and multiplied by 10^3), and energies, $\Delta E(\Omega)$, in brackets (kJ mol^{-1}) for the gauche conformer of ethylamine (**EA-*g***). Values are relative to those in the antiperiplanar conformer (**EA-*t***) (au).

in methanediol (100% of the electron density lost by H^C in ***gg*** is received by the O−C−O unit).[16]

QTAIM analysis of both ethylamine conformers (**EA-*g*** and **EA-*t***, Figure 4) reveals that both leading factors (number of *lp*−N−C−H gauche arrangements and parallel *lp*—N···X′—H^X dispositions) can also be invoked to explain $\Delta N(\Omega)$ conformational variations in simple monoamines and are not specific of anomeric compounds. In fact, there are three significant $\Delta N(\Omega)$ values in **EA-*g*** with regard to $N(\Omega)$ values in **EA-*t***. They include two depletions, which correspond to H* (the hydrogen involved in H−C···N−*lp* parallel arrangement in **EA-*g***) and the carbon of the methyl group (experiencing one gauche arrangement to the nitrogen *lp* in **EA-*g*** and none in **EA-*t***). There is also a significant increase of electron population, $\Delta N(H^{\#}) = 0.027$ au, *lp*−N−C−$H^{\#}$ passing from a gauche arrangement in **EA-*t*** to an antiperiplanar one in **EA-*g***.

In the same vein found for O−C−O containing compounds, $\Delta N(H)$ and $\Delta E(H)$ values are linearly correlated with negative fitting slopes. Therefore, negative $\Delta N(H)$ values are accompanied by energy destabilizations (positive $\Delta E(H)$ values in Figure 3). For aminic compounds, we need to consider two kinds of hydrogens (H^C and H^N), the slope of the former being steeper than that of the latter. Why does adding the same electron density reduce the energy more in H^N than in H^C? According to the energy partitioning terms, the electron density in H^N basins is, on average, less attracted by the nuclei in the molecule than in the H^C basins.

The $\Delta N(\Omega)$ versus $\Delta E(\Omega)$ linear correlation also holds for C and N atoms, with larger absolute slopes, although some clear outliers (most of them for N) can be observed (Figure S3, Supporting Information). This can be explained considering that N is the most electronegative element in the molecule. Its electron density is the least affected by conformational changes ($\Delta N(N)$ values only span in a 0.023 au range, that is, 0.3% of its averaged electron population, 7.92 au), although the electron density of N basins experience very different electric fields in each conformation. Therefore, $\Delta E(N)$ values are more affected by variations of the N environment than for $\Delta N(N)$. Ranges of $\Delta N(\Omega)$ variations indicate the important role played by electronegativity in determining the relative variations experienced by different kinds of atoms during the conformational change. Thus, the largest range corresponds to H^C (0.078 au representing more than 8% of its electron population), and it is much lower for H^N because of the proximity to a N atom (around 3% of its averaged electron density), and it is less in carbons (0.6% of its averaged electron population).

Looking at **MDA** $\Delta E(\Omega)$ values, we observe that the stabilization gained by the carbon atom in **MDA-*tt*** (−24 kJ mol^{-1}) is not enough to compensate for the destabilizations achieved by both H^C atoms (60 kJ mol^{-1} altogether). The stabilization by aminic hydrogens because of avoiding parallel

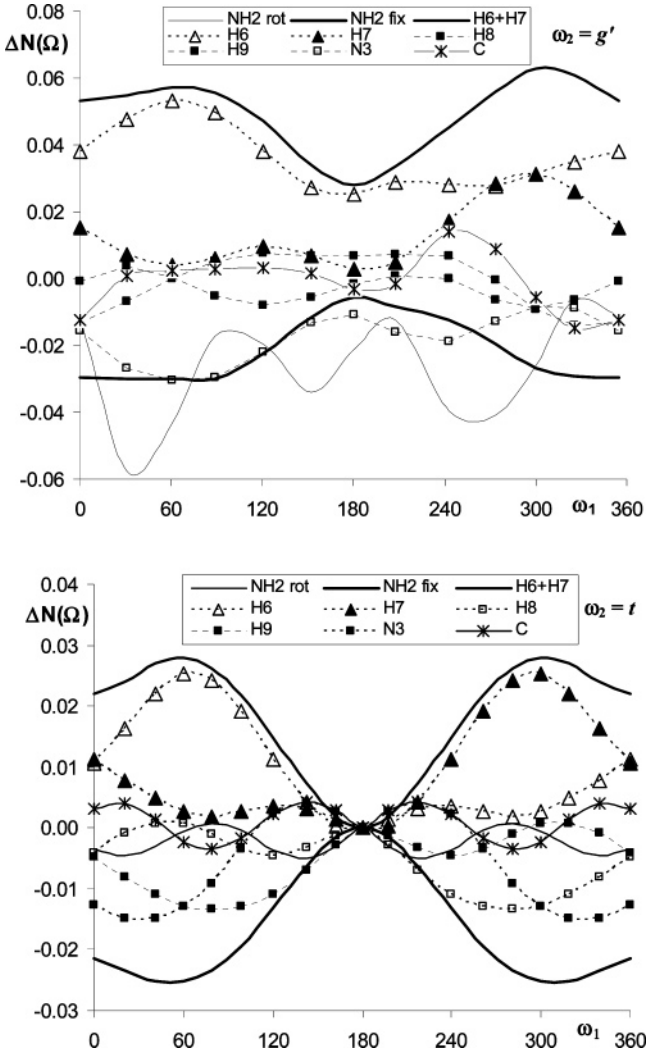

Figure 5. Evolution of the B3LYP/6-311++G(2d,2p) 6d atomic electron populations (values in au, multiplied by 10^3 and relative to those in **MDA-*gg***) along the internal rotation around the N_1-C_2 bond of methanediamine when $N_1-C_2-N_3-lp$ keeps antiperiplanar ($\omega_2 = t$) and gauche ($\omega_2 = g$) arrangements.

dispositions to *lp*s plays a crucial role (−47 kJ mol^{-1}) in the conformational preference of **MDA-*tt***. Atomic partitioning of the **MDA-*tg*** conformational energy (Figure 3) also reveals that this conformer is destabilized with regard to **MDA-*tt*** not only because of the relative destabilization of the N−C−N unit (14 kJ mol^{-1}), which does not compensate for the stabilization experienced by one of the central hydrogens ($\Delta E(H_6) = -19$ kJ mol^{-1}), but also because of the destabilization of an aminic hydrogen that achieves a *lp*—N···N—H parallel disposition ($\Delta E(H_5) = 18$ kJ mol^{-1}). Therefore, for **MDA**, the characteristic conformational preference of the anomeric effect is due to a combination of electron density transference to carbon and aminic hydrogens.

It is also important to note that data shown in Figure 3 cannot be explained with the SM. Thus, according to the SM, $\Delta N(N_4)$ should be positive for **MDA-*tg***, where the gauche arrangement of $lp-N_4-C_3-N_2$ would preclude the $n_{N4} \rightarrow \sigma^*_{C3-N2}$ electronic transfer present in **MDA-*tt***. On the contrary, we observe that $\Delta N(N_4)$ for **MDA-*tg*** is negative (Figure 3).

The variations displayed by the atomic electron populations of **MDA** along two different internal rotations are shown in Figure 5. The three computational levels considered here provide the same relative evolution (Table 2 and Figure S4 in the

TABLE 2: Relative Atomic Electron Populations,[a] with Regard to MDA-*tt*,[b] for Remaining Conformers[c] of MDA and MDA-*gg′* Conformations[d] Computed from Electron Densities Obtained at Different Computational Levels[e]

	MDA-*tg*			MDA-*gg*			MDA-*gg′*		
	HF	B3LYP	MP2	HF	B3LYP	MP2	HF	B3LYP	MP2
Δ*N*(N1)	−10	−7	−7	−10	−6	−6	−35	−27	−30
Δ*N*(N3)	−6	−2	−3	−10	−6	−6	−35	−27	−30
Δ*N*(C2)	3	−2	−2	−3	−9	−9	12	4	4
Δ*N*(H6)	6	6	5	36	32	32	6	5	5
Δ*N*(H7)	28	23	24	36	32	32	59	51	52
Δ*N*(H5)	0	−1	0	−18	−15	−16	−6	−6	−4
Δ*N*(H4)	−18	−16	−16	−7	−6	−6	3	3	4
Δ*N*(H9)	−5	−4	−3	−7	−6	−6	−6	−6	−4
Δ*N*(H8)	3	3	3	−18	−15	−16	3	3	4

[a] All values in au multiplied by 10^3. [b] Absolute values for **MDA-*tt*** are shown in Table S1 (Supporting Information). [c] Figure S4 (Supporting Information) shows the evolution of $N(\Omega)$ along ω_1 rotation for $\omega_2 = 180°$. [d] Electron density obtained from single-point calculation on the HF/6-311++G(2d,2p) 6d optimized geometry. [e] 6-311++G(2d,2p) 6d basis set used at the three levels.

Supporting Information). This led us to comment exclusively on the results obtained with B3LYP electron densities. This agreement was previously detailed for dimethoxymethane.[16]

The evolution of the atomic electron population along the C−N internal rotations (Figure 5) shows that the population of the central hydrogens (H6 + H7) and that at the fixed NH2 (N3 + H8 + H9) follow opposite trends. This agrees with the explanation presented previously for the relative atomic electron populations of the **MDA** conformers. Moreover, looking at the atomic components of both groups of electron populations, we observe that every atom displays its largest $N(\Omega)$ depletion when it is affected by the largest steric interactions: H6 when $180° \leq \omega_1 \leq 300°$, H7 when $60° \leq \omega_1 \leq 180°$ (respectively, the regions where N1 and N3 *lp*s display their closest approach to those hydrogens), H9 between 60 and 120°, and H5 between 240 and 300° (respectively, when the units *lp*—N1···N3—H9 and *lp*—N3···N1—H5 are nearly synperiplanar). Also, contrary to what should be expected according to the SM, the electron population of the rotated NH_2 group (N1 + H4 + H5) displays very little variation (less than 0.005 au) and three maxima along the internal rotation (only one, at $\omega_1 = 180°$, should appear from the $n_N \rightarrow \sigma^*_{C-N}$ transference).

It is also important to note that the variations displayed by *N*(C3) are always much smaller. This confirms that although steric effects can also be employed to explain the anomeric conformational preferences in **MDA**, the different interactions have distinct relative weights to those present in the O−C−O models. Both internal rotations (for $\omega_2 \approx 180°$ and $\omega_2 \approx 60°$) can be explained in the same terms, the only difference being that the symmetry displayed in the former makes its explanation easier.

2,2-Propanediamine. Replacement of the central hydrogens by methyl groups in **MDA** led to several changes in the conformational trends. Thus, in **PDA**, we observed that the relative energies of conformers were reduced and that **PDA-*gg′*** was obtained as a minimum on the B3LYP/6-311++G(2d,2p) 6d energy surface (Table 1). **PDA-*tt*** is the most stable conformer, although its electronic molecular energy is only 0.2 kJ mol^{-1} more negative than those of **PDA-*gg*** and **PDA-*tg***, which is below the confidence limit for this computational level. To the best of our knowledge, there is no other experimental or computational conformational analysis on this system. Therefore, we assume that these three conformers are nearly isoenergetic, whereas **PDA-*gg′*** is significantly destabilized with regard to them (Table 1). It should be stressed that the anomeric

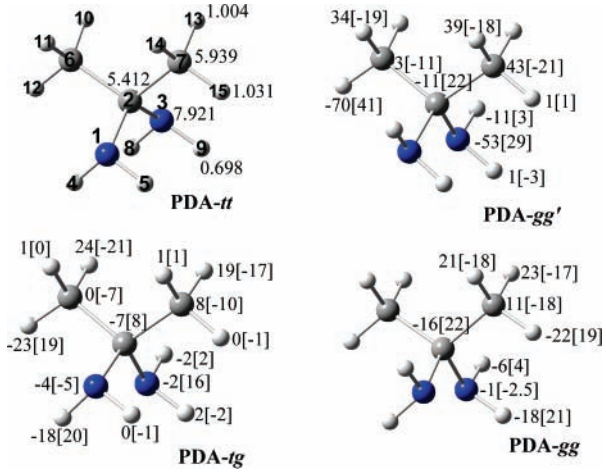

Figure 6. Structure and atom numbering of the conformers of 2,2-propanediamine (**PDA**). Absolute $N(\Omega)$ values (for **PDA-*tt***) are in au. Relative atomic electron populations, $\Delta N(\Omega)$, for the remaining conformers in au and multiplied by 10^3. $\Delta E(\Omega)$ values relative to atomic energies in **PDA-*tt*** are shown in brackets (kJ mol^{-1}). All values were obtained from B3LYP/6-311++G(2d,2p) calculations. **PDA-*tt***, **PDA-*tg***, **PDA-*gg*,** and **PDA-*gg′*** full optimized geometries display, respectively, C_{2v}, C_1, C_2, and C_s symmetries.

conformational preference for ***tt*** is significantly reduced from **MDA** to **PDA** (from 1.4 to 0.2 kJ mol^{-1}, Table 1), something that cannot be predicted on the basis of the SM.

The comparison of the atomic populations of the ***gg*** and ***tt*** conformers is basically equivalent to that presented for **MDA**. Thus, the electron density gained by each methyl group in **PDA-*gg*** with regard to **PDA-*tt*** (0.033 au) is practically the same as that obtained by each H^C in **MDA-*gg*** (0.032 au). Nevertheless, the stabilization gained by a methyl group in **PDA-*gg*** (−34 kJ mol^{-1}) is a little bit larger than that observed for H^C in **MDA-*gg*** (−30 kJ mol^{-1}). The largest difference in the $\Delta N(\Omega)$ values (computed as **PDA-*gg*** − **PDA-*tt***) corresponds to the central carbon, C2, which loses electron density more (0.007 au) in **PDA-*gg*** than in **MDA-*gg***. In spite of this rather significant difference of ΔN(C2) values, ΔE(C2) is only 2 kJ mol less in **PDA** than in **MDA**. Finally, ΔN and ΔE values for the NH_2 groups do not differ by more than 0.002 au and 2 kJ mol^{-1}, respectively. Overall, looking at the $\Delta E(\Omega)$ and $\Delta N(\Omega)$ values, we can relate the decrease experienced by the relative energy of ***gg*** in **PDA** to the electron density gained by the carbons of the methyl groups in **PDA-*gg*** (0.011 au each that stabilize every carbon by 18 kJ mol^{-1}).

A similar comparison can be established between **PDA-*tg*** and **MDA-*tg***, concluding that methyl groups replace H^Cs with no important differences for $\Delta N(\Omega)$ but add a slight stabilization because of the electron density gained by the methylic carbon C7, which does not experience *lp*−N−C−C gauche arrangements.

Two important electron density transferences can be considered according to $\Delta N(\Omega)$ values shown for **PDA-*tg*** in Figure 6. One from H12 to H10, originating from their distances to N3 *lp*, H12 being the closest and H10 the furthest. Another one sends electron density from the aminic hydrogen that is parallel to N3 *lp*, H4, to the C7 methyl group, as it has one less *lp*−N−C-C7 gauche disposition in **PDA-*tg*** than in **PDA-*tt***.

Finally, in **PDA-*gg′***, H12 is close to the two *lp*s, resulting in a very large electron density transfer (0.070 au) to the other two hydrogens of this methyl group. Nitrogen *lp*s are parallel in this conformer. This interaction can be related to very

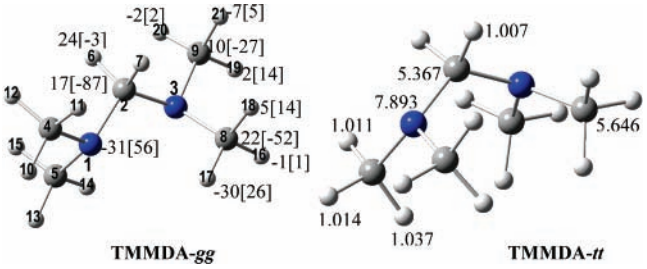

Figure 7. Structure and atom numbering of the C_2 (**TMMDA-*gg***) and C_{2v} (**TMMDA-*tt***) conformers of *N*,*N*′,*N*′,*N*′-tetramethylmethanediamine (**TMMDA**). Absolute $N(\Omega)$ values (for **TMMDA-*tt***) are in au. Relative atomic electron populations, $\Delta N(\Omega)$, for **TMMDA-*gg*** are in au and multiplied by 10^3. $\Delta E(\Omega)$ values relative to atomic energies in **TMMDA-*tt*** are shown in brackets (kJ mol^{-1}). All values were obtained from B3LYP/6-311++G(2d,2p) calculations.

significant N(N) reductions (0.053 au per N basin) and a slight reduction of N(C2). The electron density is gained by C8, which has no *lp*−N−C−C8 gauche arrangement. Basically, the high relative energy of **PDA-*gg′*** comes from the destabilization experienced by aminic groups and C2, which is not compensated by the stabilization of the methyl groups.

N*,*N*,*N*′,*N*′-Tetramethylmethanediamine.** When all the aminic hydrogens of **MDA** are replaced by methyl groups, the anomeric conformational preference is inverted, and **TMMDA-*gg is more stable than **TMMDA-*tt*** (Table 1). The latter conformer displays C_{2v} symmetry with four equivalent methyl groups, whereas the former is C_2, showing two different sets of methyl groups. We will refer to them as inner (C10 and C14) and outer (C6 and C18), the latter being closer to the *lp* of the N which they are not attached.

In this case, the variation of steric interactions in the conformational change gives rise to important electron density transferences. Thus, the closest hydrogens to each N *lp* (H11 and H17) experience important depletions of electron population in **TMMDA-*gg***, whereas the carbons attached to them show positive ΔN(C) values (Figure 7). These transferences stabilize outer methyl groups (around 11 kJ mol^{-1} each). The N atoms are less populated in **TMMDA-*gg*** than in **TMMDA-*tt***, whereas the central methylene (at C2) increases its population (Figure 7). As a result of this transference, the summation of atomic energies of the N−CH$_2$−N unit is 19 kJ mol^{-1} less negative in **TMMDA-*gg***. Overall, the conformational preference for **TMMDA-*gg*** comes from the stabilization of all the methyl groups (more those in the outer than those in the inner disposition). It exceeds the destabilization experienced by N−CH$_2$−N. The significant negative ΔN(N) values displayed by **TMMDA-*gg*** were only observed in the molecules shown previously in one case (**PDA-*gg′***). In both cases, the steric interactions can be considered to be high because of the proximity between the *lp*s of both N atoms (**PDA-*gg′***) or due to the proximity of each *lp* to an outer methyl group.

1,3-Diazacyclohexane and 1,3,5-Triazacyclohexane. To complete our study, we have also considered three anomeric saturated heterocycles. The relative atomic electron populations of their conformers are conditioned by the same steric effects commented on previously. That is, an increased number of *lp*−N−C−H gauche arrangements and *lp*—N···X—H (X═C, N) parallel dispositions (in this case, also named *lp*···H diaxial interactions) produce electron depletions in the hydrogen basin. *lp*—N···X—H (X═C, N) parallel dispositions also reduce N(X). Finally, the *lp*···*lp* diaxial interactions have to be considered as another depleting factor of N(N) values.

Thus, the diequatorial conformer (**DAC-*g′g***) displays $N(\Omega)$ depletions (with regard to **DAC-*tt***) at H5^{ax} and C5, due to two

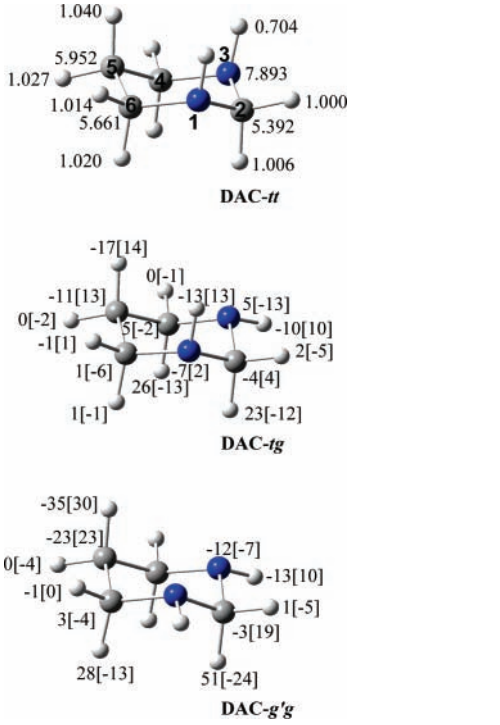

Figure 8. Structure and atom numbering of the conformers of 1,3-diazacyclohexane (**DAC**). Absolute $N(\Omega)$ values (for **DAC-*tt***) are in au. Relative atomic electron populations, $\Delta N(\Omega)$, for the remaining conformers are in au and multiplied by 10^3. $\Delta E(\Omega)$ values relative to atomic energies in **DAC-*tt*** are shown in brackets (kJ mol^{-1}). All values were obtained from B3LYP/6-311++G(2d,2p) calculations. **DAC-*tt***, **DAC-*tg***, and **DAC-*gg′*** full optimized geometries display, respectively, C_2, C_1, and C_2 symmetries.

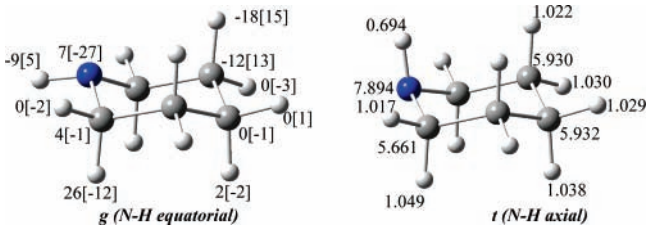

Figure 9. Relative atomic electron populations, $\Delta N(\Omega)$ (in au and multiplied by 10^3), and energies, $\Delta E(\Omega)$, in brackets (kJ mol^{-1}) for the N−H equatorial conformer (***g***) of piperidine. Values are relative to those in the N−H axial conformer (***t***).

lp···H diaxial interactions, and at both Ns due to the *lp*···*lp* diaxial interaction (Figure 8). The electron density lost by these basins is transferred to H2^{ax}, H4^{ax}, and H6^{ax}, which have lost *lp*−N−C−H gauche interactions with regard to **DAC-*tt***.

The features governing the electron density evolution of N−C−N containing compounds can also be observed in simple cyclic amines. Thus, looking at piperidine (Figure 9), we observe that the change of the electron density of the CH$_2$ groups (global electron density transference from C−H^{ax} in β to C−H^{ax} in α) can be successfully explained considering that *lp*···H diaxial and *lp*−N−C−H gauche interactions play an electron withdrawal role on the H basins. Nevertheless, $\Delta E(\Omega)$ values associated with these $\beta \rightarrow \alpha$ electron transferences would destabilize the ***g*** conformer with regard to the ***t*** one. In fact, N stabilization in the ***g*** conformer (27 kJ mol^{-1}) is essential for the conformational preference. According to the partitioning of the atomic energy, N with an axial *lp* becomes stabilized with regard to those with equatorial *lp*s because the electron density contained within the N basin with an axial *lp* experiences larger nuclear attractions (2682 kJ mol^{-1}), which exceed the also

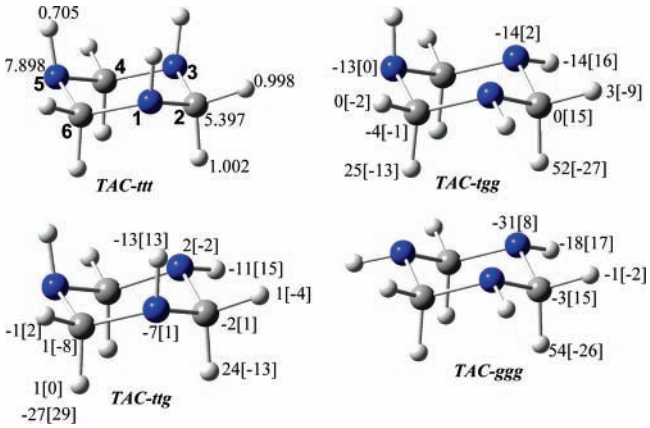

Figure 10. Structure and atom numbering of the conformers of 1,3,5-triazacyclohexane (**TAC**). Absolute $N(\Omega)$ values (for **TAC-*ttt***) are in au. Relative atomic electron populations, $\Delta N(\Omega)$, for the remaining conformers are in au and multiplied by 10^3. $\Delta E(\Omega)$ values relative to atomic energies in **TAC-*ttt*** are shown in brackets (kJ mol^{-1}). All values were obtained from B3LYP/6-311++G(2d,2p) calculations. **TAC-*ttt***, **TAC-*ttg***, **TAC-*tgg′***, and **TAC-*g′gg′*** full optimized geometries display, respectively, C_2, C_1, C_1, and C_2 symmetries.

increased electron−electron repulsions (2625 kJ mol^{-1}). It should be mentioned that this is only true with total atomic electron densities but not for averaged electrostatic potentials (referred to 1 au) experienced by the N basin. Therefore, the stabilization of the *lp* axial N atom is also associated with gaining some electron density from the equatorially attached H basin (0.009 au are transferred from the aminic hydrogen in ***g*** with regard to ***t***). Therefore, we need to consider another factor when studying cyclic azacompounds: the stabilization gained by N with axial *lp* and an associated electron transference from the attached aminic H. Nevertheless, this associated electron transference can be hidden in the N basin by a *lp*···*lp* diaxial interaction in polyaza compounds, as is seen in **DAC-*g′g***.

Considering the proximity between electron density sources and drains, the transference from C5 and H5^{ax} to H4^{ax} and H6^{ax} destabilizes **DAC-*g′g*** more than the stabilization provided by the transference from the N−H groups to H2^{ax} (Figure 8). N(C5) depletion due to axial *lp*s plays an important role in this balance destabilizing the **DAC-*g′g*** conformer.

According to the previous explanation, electron reorganization in **DAC-*tg*** (with regard to **DAC-*tt***) should present smaller N(H5^{ax}) and N(C5) depletions (there is only one *lp*···H5^{ax} diaxial interaction), and we should only observe a depletion for N(N1) but not for N(N3). At the same time, the electron population gained by H2^{ax} should be less than in **DAC-*g′g*** (one gauche interaction less), and N(H4^{ax}) should increase but not N(H6^{ax}). This is what we find looking at $\Delta N(\Omega)$ values presented in Figure 8.

The relative energy increases with the number of equatorial *lp*s, as was previously found at the HF level[37] and contrary to MM2(80) calculations.[38] Thus, the triaxial conformer (**TAC-*ttt***) (Figure 10) has the most negative energy (Table 1). This stabilization can be explained as due to the electron density transferred from axial hydrogens (0.050 au from every H) to N−H groups when the former experiences *lp*−N−C−H gauche interactions.

2-Aminopiperidine. Twelve initial conformations were fully optimized for this molecule. They are named with three-character acronyms, where the first and third characters indicate, respectively, the arrangements of the *lp*−N1−C2−N7 and *lp*−N7−C2−N1 dihedral angles (Figure 11): ***t*** for antiperiplanar, ***g*** for clockwise gauche, and ***g′*** for counterclockwise gauche.

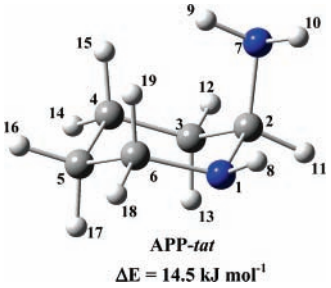

Figure 11. Optimized structure, atom numbering, and relative energy (with regard to the most stable conformer) for the ***tat*** conformer 2-aminopiperidine (**APP-*tat***).

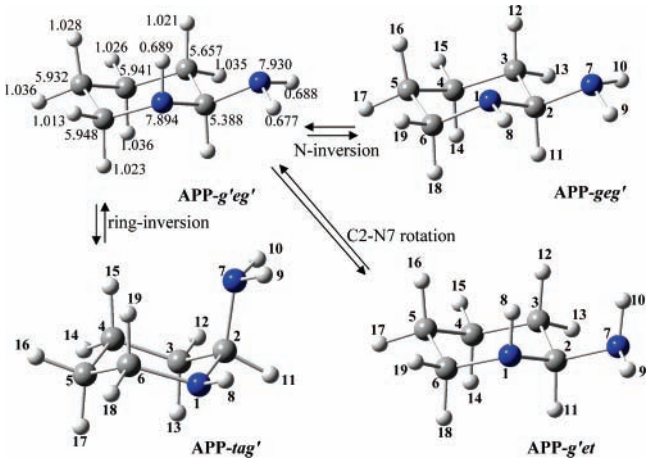

Figure 12. Absolute $N(\Omega)$ values obtained from B3LYP/6-311++G-(2d,2p) calculations for the most stable conformer (**APP-*g′eg′***) are in au. Optimized structures for the conformers were obtained by direct interconversion from **APP-*g′eg′***.

The second character denotes whether the NH_2 group at C2 is oriented axially (***a***) or equatorially (***e***). Eleven of these initial conformations (all but ***g′eg***) were obtained as different conformers whose relative molecular energies are listed in Table 3. It is remarkable that according to SM, **APP-*tat*** (Figure 11) should be the most stable conformer. Nevertheless, seven conformers of **APP** display more negative energies (Table 3).

Again, the relative energies of the conformers are explained considering the electron density transferences among atoms associated with the same steric interactions employed in the previous molecules (Table 3). For the sake of concision, we will only comment on the three one-step conformational changes that **APP-*g′eg′*** can experience: N1 inversion, chair inversion, and C2−NH2 internal rotation (Figure 12).

N1 inversion transforms **APP-*g′eg′*** into **APP-*geg′***. This process replaces two H···H diaxial interactions (H10···H12 and H10···H16) by *lp*···H ones, depleting N(H12), N(C3), N(H16), and N(C5) (0.059 au in total, Table 4). At the same time, *lp*−N1−C2−H11 and *lp*−N1−C6−H18 gauche arrangements become antiperiplanar ones, which allows increasing N(H18) and N(H11) (0.046 au in total or 0.057 including also N(C2) and N(C6) enlargements). These variations can be described basically as electron transferences along two H^{ax}−C−C−H^{ax} units (H12−C3−C2−H11 and H16−C5−C6−H18). Although most of the global change corresponds to axial hydrogens, the carbons connecting them are also affected because the reorganization of the electron density is continuous, as previously shown even for several models of π-delocalized compounds.[39] Finally, the parallel *lp*—N1···N7—H8 orientation of **APP-*g′eg′*** turns into a parallel H10—N1···N7—H8 orientation in **APP-*geg′*** after N1 inversion. The result is a relative increase of N(H8)

TABLE 3: B3LYP/6-311++G(2d,2p) 6d Relative Total Electronic Molecular Energies (kJ mol^{-1}) with Regard to Most Stable Conformer (*g′eg′*, $E = -307.36765$ au) and Relative Values of Group Energies (kJ mol^{-1}) with Regard to Their Corresponding Values in *g′eg′*[a]

	geg	*geg′*	*get*	*g′et*	*g′ag*	*g′ag′*	*g′at*	*tag′*	*tag*	*tat*
ΔE	3.7	10.4	3.1	0.2	32.6	7.8	19.5	7.3	7.7	14.5
CH(2)	15	−4	17	7	74	19	46	13	22	43
CH_2(3)	−35	20	38	14	−48	−1	36	23	15	59
CH_2(4)	−14	1	6	−1	−10	3	−10	0	−17	−18
CH_2(5)	22	24	26	−1	6	−3	5	19	21	30
CH_2(6)	−9	−16	−26	−9	−11	−7	−29	−19	−30	−45
NH(1)	20	−20	−67	−1	32	16	−27	−15	5	−42
NH_2(1)	8	5	10	−6	−11	−17	−2	−15	−6	−13

[a] See Figure 12 for atom numbering.

TABLE 4: B3LYP/6-311++G(2d,2p) 6d Relative Atomic Electron Populations (in au and Multiplied by 10^3) with Regard to Their Corresponding Values in Most Stable Conformer (*g′eg′*)[a]

	geg	*geg′*	*get*	*g′et*	*g′ag*	*g′ag′*	*g′at*	*tag′*	*tag*	*tat*
N1	4	−10	5	−4	−16	−1	−1	7	1	16
C2	9	8	15	4	2	4	13	13	12	18
C3	−12	−10	−16	−5	1	−6	−6	−17	−9	−16
C4	3	−1	−2	0	0	−2	−1	−3	0	−2
C5	−12	−12	−13	0	0	−2	−1	−14	−12	−12
C6	2	3	8	7	1	5	5	5	5	5
N7	0	−15	−6	−3	−14	−5	0	−7	−1	−2
H8	−9	7	12	21	8	9	19	9	−6	11
H9	10	18	0	19	16	0	15	22	14	14
H10	−8	−2	9	−11	1	4	−12	7	9	9
H11	−7	20	−11	−24	−32	−1	−33	−8	−27	−39
H12	6	−17	4	22	15	13	−12	15	12	−10
H13	1	1	−22	−23	10	2	4	−16	−16	−14
H14	2	1	0	−2	−11	−4	−13	−4	−11	−13
H15	3	0	0	0	16	−10	12	−7	19	15
H16	−14	−18	−14	3	−7	−7	−6	1	1	2
H17	1	1	1	−1	8	15	9	−10	−15	−16
H18	24	26	26	−2	−13	−4	−12	−2	−9	−11
H19	−1	0	3	1	14	−11	19	10	34	44

[a] See Figure 12 for atom numbering and atomic electron populations of **APP-*g′eg′***.

in **APP-*geg′***, which gains electron density from attached N7 (involved now in a diaxial *lp*···*lp* interaction, which reduces the electron density of the N basin). This diaxial *lp*···*lp* interaction facilitates reducing both N(N7) and N(N1) (0.015 and 0.010 au, respectively). Looking at $\Delta E(\Omega)$ values, we realize that H^{ax}−C3−C2−H^{ax} and H^{ax}−C5−C6−H^{ax} transferences are destabilizing (16 and 8 kJ mol^{-1} respectively), as well as the inversion of N1 destabilizing in 5 kJ mol^{-1}, whereas reorganizing the electron density of the NH_2 group reduces its energy by 20 kJ mol^{-1}. In contrast, the energy of the CH_2 group at C4 (the only one not involved in electron density transferences or reorganizations) is practically the same in both conformers (Table 3). Overall, there is an important decrease of $N(\Omega)$ for heavy atoms (−0.037 au) that gives rise to a rather destabilized conformer (10.4 kJ mol^{-1})

Internal rotation around the C2−N7 bond transforms **APP-*g′eg′*** into **APP-*g′et***. Six significant modifications of $N(\Omega)$ can be observed in Table 4 for this conformational change. The three largest $N(\Omega)$ enhancements are presented by those hydrogens that leave a *lp*—N···N—H parallel disposition: H8, H11, and H12. In contrast, the largest $N(\Omega)$ depletions correspond to the two hydrogens that become parallel to *lp*−N units (H9 and H13), and to H11, which passes from an antiperiplanar to a gauche *lp*−N7−C2−H11 arrangement. Looking at Table 3, we can observe that the energy of no structural units varies significantly because of this process and that both conformers are practically isoenergetic. This is reasonable, if we take into account that the only $\Delta N(\Omega)$ significant values correspond to H atoms, whereas the total population of heavy atoms remains nearly constant (−0.001 au).

Ring inversion of **APP-*g′eg′*** turns it into **APP-*tag′***. Table 4 shows that the main enhancements of $N(\Omega)$ accompanying this interconversion correspond to hydrogens that lose a H—C···N—*lp* parallel disposition (H9, H12, and H8, the latter is smaller as it is bonded to an electronegative atom) or to hydrogens that lose a H−C−N−*lp* gauche arrangement (H19). The largest depletions are shown by hydrogens that gain a H—C···N—*lp* parallel disposition (H13 and H17) and by the ring atoms attached to them (C3 and C5). Overall, we observe that 0.016 au are transferred from heavy atoms to hydrogens, giving rise to an intermediate destabilization for this conformer (7.3 kJ mol^{-1}).

Conclusion

The evolution of QTAIM computed atomic electron populations along the internal rotations of methanediamine and the changes experienced by them among the conformers of other model compounds containing the N−C−N anomeric unit (2,2-propanediamine, *N,N,N′,N′*-tetramethylmethanediamine, 2-aminopiperidine, 1,3-diazacyclohexane, and 1,3,5-triazacyclohexane) are not in line with the stereoelectronic model of the anomeric effect. In contrast, these variations can be explained on the basis of steric interactions. This interpretation is similar to that recently proposed by our group for the O−C−O unit, although some particularities of the N−C−N unit have to be taken into account. Thus, preferred conformers are conditioned by two factors: (i) the reduction of the electron population experienced by the hydrogens of the central methylene when they display more gauche arrangements to lone pairs and (ii) the reduction of the electron population of aminic hydrogens when the corresponding N−H bond is in parallel arrangement to the lone pair of another N (diaxial orientation in azacyclohexanes). The former depletion takes place in *lp*−N−C−N antiperiplanar dispositions, whereas the latter is shown in *lp*−N−C−N gauche arrangements. Therefore, we can say that the electron density removed from the central hydrogens is moved to an aminic hydrogen on going from an antiperiplanar to a gauche position of the *lp*−N−C−N unit. The relative energies of aminic and central hydrogens in the conformer series are the main factor determining the conformational preference. This is in contrast to what happens in O−C−O containing compounds, where both N(H) depletions take place in O−C−O−H gauche dispositions and the electron density removed from H basins is transferred to heavy atoms (C and O). Therefore, the stabilization gained by N and C atoms plays a secondary role in most of the models considered here. This also explains why the anomeric conformational stabilization due to N−C−N units is significantly less than that of O−C−O− units. This is in line with a

general trend exhibited by hydrogens as the most available (less energy cost) atomic basins for receiving or providing electron density along a chemical change.[40]

Taking into account that QTAIM atomic properties are computed from electron densities, whereas NBO results that support the hyperconjugative model are based upon MOs, we believe that the data we are using are less affected by all the approximations included in the molecular orbital theory. In fact, MOs are used in QTAIM with the sole purpose of enabling the calculation of electron density.[41] On the contrary, the NBO analysis is based on the significance of molecular orbitals.

Acknowledgment. This work was funded by the Spanish MEC through Project CTQ2006-15500/BQU. We are also indebted to the Centro de Supercomputación de Galicia (CESGA) for providing free access to its computational facilities. K.E. thanks the Iranian Ministry of Science, Research and Technology for a fellowship funding his stay at Vigo University.

Supporting Information Available: Figures of electronic molecular energy evolution, gauche interactions in methanediol and methanediamine, plots of $\Delta N(\Omega)$ vs $\Delta E(\Omega)$ for conformers of linear molecules, and evolution of atomic electron populations obtained at different computational levels. Table of atomic electron populations of **MDA-*tt***. This material is available free of charge via the Internet at http://pubs.acs.org.

References and Notes

(1) Thacher, G. R. J. *The Anomeric Effect and Associated Steroelectronic Effects*; ACS Symposium Series No. 539; American Chemical Society: Washington, DC, 1993.
(2) Kirby, J. *The Anomeric Effect and Related Stereoelectronic Effects of Oxygen*; Springer-Verlag: Berlin, 1983.
(3) Deslongchamps, P. *Stereoelectronic Effects in Organic Chemistry*; Wiley: New York, 1983.
(4) Juaristi, E.; Cuevas, G. *The Anomeric Effect*; CRC Press: Boca Raton, FL, 1995.
(5) Edward, J. T. J. *Chem. Ind.* **1955**, 1102.
(6) Suárez, D.; Sordo, T. L.; Sordo, J. A. *J. Am. Chem. Soc.* **1996**, *118*, 9850.
(7) Tvaroska, I.; Bleha, T. *Advances in Carbohydrate Chemistry and Biochemistry*; Academic Press: San Diego, 1989; Vol. 47, p 107.
(8) Romers, C.; Altona, C.; Buys, H. R.; Havinga, E. *Top. Stereochem.* **1969**, *4*, 39.
(9) Carballeira, L.; Pérez-Juste, I. *J. Comput. Chem.* **2000**, *21*, 462.
(10) Salzner, U.; Schleyer, P. v. R. *J. Am. Chem Soc.* **1993**, *115*, 10231.
(11) Salzner, U.; Schleyer, P. v. R. *J. Org. Chem.* **1994**, *59*, 2138.
(12) Carballeira, L.; Pérez-Juste, I. *J. Comput. Chem.* **2001**, *22*, 135.
(13) Grein, F.; Deslongchamps, P. *Can. J. Chem.* **1992**, *70*, 604.
(14) Grein, F.; Deslongchamps, P. *Can. J. Chem.* **1992**, *70*, 1562.
(15) Chang, Y.-P.; Su, T.-M. *J. Mol. Struct.* **1996**, *365*, 183.
(16) Vila, A.; Mosquera, R. A. *J. Comput. Chem.* **2007**, *28*, 1516.
(17) Bader, R. F. W. *Atoms in Molecules, A Quantum Theory; International Series of Monographs in Chemistry, No. 22*; Oxford University Press: New York, 1990.
(18) Bader, R. F. W. *Chem. Rev.* **1991**, *91*, 893.
(19) Werstiuk, N. H.; Laidig, K. E.; Ma, J. In *Anomeric Effects and Associated Stereoelectronic Effects*; Thatcher, G. J. R., Ed.; ACS Symposium Series No. 539; American Chemical Society: Washington, DC, 1993; p 176.
(20) Vila, A.; Mosquera, R. A. *Chem. Phys. Lett.* **2007**, *443*, 22.
(21) Frisch, M. J.; Trucks, G. W.; Schlegel, H. B.; Scuseria, G. E.; Robb, M. A.; Cheeseman, J. R.; Montgomery, J. A., Jr.; Vreven, T.; Kudin, K. N.; Burant, J. C.; Millam, J. M.; Iyengar, S. S.; Tomasi, J.; Barone, V.; Mennucci, B.; Cossi, M.; Scalmani, G.; Rega, N.; Petersson, G. A.; Nakatsuji, H.; Hada, M.; Ehara, M.; Toyota, K.; Fukuda, R.; Hasegawa, J.; Ishida, M.; Nakajima, T.; Honda, Y.; Kitao, O.; Nakai, H.; Klene, M.; Li, X.; Knox, J. E.; Hratchian, H. P.; Cross, J. B.; Bakken, V.; Adamo, C.; Jaramillo, J.; Gomperts, R.; Stratmann, R. E.; Yazyev, O.; Austin, A. J.; Cammi, R.; Pomelli, C.; Ochterski, J. W.; Ayala, P. Y.; Morokuma, K.; Voth, G. A.; Salvador, P.; Dannenberg, J. J.; Zakrzewski, V. G.; Dapprich, S.; Daniels, A. D.; Strain, M. C.; Farkas, O.; Malick, D. K.; Rabuck, A. D.; Raghavachari, K.; Foresman, J. B.; Ortiz, J. V.; Cui, Q.; Baboul, A. G.; Clifford, S.; Cioslowski, J.; Stefanov, B. B.; Liu, G.; Liashenko, A.; Piskorz, P.; Komaromi, I.; Martin, R. L.; Fox, D. J.; Keith, T.; Al-Laham, M. A.; Peng, C. Y.; Nanayakkara, A.; Challacombe, M.; Gill, P. M. W.; Johnson, B.; Chen, W.; Wong, M. W.; Gonzalez, C.; Pople, J. A.; *Gaussian 03*, revision C.02; Gaussian, Inc.: Pittsburgh, PA, 2004.
(22) Biegler-König, F. W.; Bader, R. F. W.; Tang, T.-H. *J. Comput. Chem.* **1982**, *13*, 317.
(23) *AIMPAC: A Suite of Programs for the Theory of Atoms in Molecules*; Bader, R. F. W. et al., Eds.; McMaster University: Hamilton, ON.
(24) Graña, A. M.; Mosquera, R. A. *J. Chem. Phys.* **1999**, *110*, 6606.
(25) Aicken, F. M.; Popelier, P. L. A. *Can. J. Chem.* **2000**, *78*, 415.
(26) Vila, A.; Carballo, E.; Mosquera, R. A. *Can. J. Chem.* **2000**, *78*, 1535.
(27) Vila, A.; Mosquera, R. A. *J. Chem. Phys.* **2001**, *115*, 1264.
(28) López, J. L.; Mandado, M.; Graña, A. M.; Mosquera, R. A. *Int. J. Quantum Chem.* **2002**, *86*, 190.
(29) Mandado, M.; Vila, A.; Graña, A. M.; Mosquera, R. A.; Cioslowski, J. *Chem. Phys. Lett.* **2003**, *371*, 739.
(30) Cortes-Guzmán, F.; Bader, R. F. W. *Chem. Phys. Lett*. **2003**, *379*, 183.
(31) Lehd, M.; Jensen, F. *J. Comput. Chem.* **1991**, *12*, 1089.
(32) Henn, J.; Ilge, D.; Leusser, D.; Stalke, D.; Engels, B. *J. Phys. Chem. A* **2004**, *108*, 9442.
(33) Carballeira, L.; Mosquera, R. A.; Rios, M. A. *J. Mol. Struct.* **1988**, *176*, 89.
(34) Chang, Y.-P.; Su, T.-M. *J. Mol. Struct.* **1996**, *365*, 183.
(35) Blair, J. T.; Stevens, J. *Heterocycles* **1994**, *37*, 1473.
(36) González-Moa, M. J.; Mosquera, R. A. *J. Phys. Chem. A* **2003**, *107*, 5361.
(37) Carballeira, L.; Fernández, B.; Mosquera, R. A.; Ríos, M. A.; Rodríguez-Otero, J.; Vázquez, S. A. *J. Mol. Struct.* **1990**, *205*, 223.
(38) Carballeira, L.; Mosquera, R. A.; Ríos, M. A. *J. Mol. Struct.* **1989**, *195*, 89.
(39) González-Moa, M. J.; Mosquera, R. A. *J. Phys. Chem. A* **2005**, *109*, 3682.
(40) Stutchbury, N. C. J.; Cooper, D. L. *J. Chem. Phys.* **1983**, *79*, 4967.
(41) Bader, R. F. W. *Int. J. Quantum. Chem.* **2003**, *94*, 173.